Gold Fluorides

DOI: 10.1002/anie.201205072

Investigation of Gold Fluorides and Noble Gas Complexes by Matrix-Isolation Spectroscopy and Quantum-Chemical Calculations**

*Xuefeng Wang, Lester Andrews, Knut Willmann, Felix Brosi, and Sebastian Riedel**

Gold fluorides have long been known, ever since Moissan, the discoverer of the element fluorine, reported the first reaction of fluorine with gold in 1889.[1] Despite the early synthesis of AuF_3, the chemistry of gold fluorides has been explored less over the years when compared with its heavier homologues chlorine, bromine, and iodine. This is probably due to difficulties in the practical handling of the element fluorine.

The most prominent oxidation state in gold chemistry is +III, as represented by AuF_3 and higher oligomers Au_2F_6 and Au_3F_9, which have been extensively investigated experimentally[2–5] and theoretically.[6,7] Gas-phase electron diffraction (GED) experiments of the monomer have shown that this compound forms an almost T-shaped structure, owing to first-order Jahn–Teller distortion,[2] whereas a helical structure was determined for its crystal.[3,8] The planar dimer structure Au_2F_6 with two bridging fluorine atoms was also studied in the gas phase.[2,6] Similar bridging of fluorine has been observed in the dimerization and trimerization of AuF_5 to form $[Au_2F_{10}]$[9,10] and $[Au_3F_{15}]$.[10,11] This unusually high oxidation state of +V, when compared with its lighter homologues silver and copper, is due to the relativistic maximum of gold.[12–14]

To date no higher oxidation state for gold has been experimentally observed, as the previous claims of $Au^{VII}F_7$[15] have been shown by quantum-chemical calculations to be erroneously assigned[11] and they most likely correspond to $AuF_5\cdots F_2$.[16] Such quantum-chemical calculations, which consider relativistic effects as well as electron correlation, are powerful methods, especially because vibrational spectroscopy is limited because of the 100% occurrence of the natural isotopes ^{197}Au and ^{19}F.

The stability of AuF was first predicted by Schwerdtfeger[17,18] and afterwards experimentally confirmed by mass spectrometry[19,20] and microwave spectroscopy.[21] The latter method was successfully used for the discovery of the heavy noble-gas gold fluoride compounds such as NgAuF (Ng=Ar, Kr, Xe),[22–24] which have also been investigated computationally.[25,26] The corresponding neon species NeAuF has only been explored by quantum-chemical calculations,[27–29] which indicate that the bonding nature is more electrostatic and its dissociation energy is extrapolated to be 10 kJ mol^{-1}.[29]

The abovementioned gold fluorides AuF, AuF_3, and AuF_5 are closed-shell species (for complete overviews, see Pyykkö[30–32] and Mohr[33]). To the best of our knowledge, no binary open-shell gold fluorides such as AuF_2, AuF_4, or even AuF_6 have been experimentally observed. The oxidation state Au^{II} is only known if stabilized by, for example, SbF_6^- as in $[Au(SbF_6)_2]$[34] or by its polymeric mixed-valence gold(II)/gold(III) compounds $[Au_3F_8](SbF_5)_2$ and $[Au_3F_7](SbF_5)_3$.[35] However, AuH_2 has been characterized by matrix IR spectra and electronic structure computations.[36]

Herein we report IR spectra and quantum-chemical calculations of the products of laser-ablated gold atom reactions with fluorine in excess argon and neon during condensation at 4 K. New gold fluoride species were prepared by co-deposition of gold atoms with F_2/Ne or F_2/Ar mixtures onto a CsI window at 4 K[37–39] in Virginia and Freiburg. IR spectra in the Au–F stretching frequency region produced by Au atom reactions with 3, 6, 12, and 24% F_2 in argon are shown in Figure 1.

The spectra show seven major bands in the region from 730 to 470 cm^{-1}. New bands at 575.1 and 640.1 cm^{-1} decrease upon sample annealing up to 40 K, while a band at 646 cm^{-1} gives way to a nearby feature increasing at 655 cm^{-1} during annealing of the sample, along with a band at 489 cm^{-1}. Broader bands at 690 and 708 cm^{-1} also increase during annealing. The spectra in Figure 1 clearly show increasing higher frequency band intensities with increasing F_2 concentration and on sample annealing to successively higher matrix temperatures. Another 6% F_2 matrix was co-deposited with double the laser energy as estimated from the target plume intensity, and the 655 and 489 cm^{-1} bands were stronger relative to the other product absorptions, which suggests that the latter bands are due to a species with more gold atoms than the others. Finally, argon matrix spectra recorded at Virginia (Supporting Information, Figure S1) are in agreement with these results, except for a broad band at 720 cm^{-1} for the highest frequency product absorption.

[*] Prof. X. Wang
Department of Chemistry
Tongji University, Shanghai 200092 (China)
Prof. X. Wang, Prof. Dr. L. Andrews
Department of Chemistry, University of Virginia
Charlottesville, Virginia 22904-4319 (USA)
Prof. Dr. L. Andrews, K. Willmann, Dipl.-Chem. F. Brosi, Dr. S. Riedel
Institut für Anorganische und Analytische Chemie
Albert-Ludwigs-Universität Freiburg
Albertstrasse 21, 79104 Freiburg im Breisgau (Deutschland)
E-mail: sebastian.riedel@psichem.de
Homepage: www.psichem.de

[**] Financial support from the NSF (Grant CHE 03-52487), a DAAD Research Visit to Freiburg for L.A., and an NSFC Grant (20973126) to X.W. is acknowledged. S.R. thanks the DFG project HA 5639/3-1 and the Fonds der Chemischen Industrie for financial support, the BWGrid cluster for computational resources, and Prof. I. Krossing and Prof. H. Hillebrecht for their generous and continuous support.

Supporting information for this article is available on the WWW under http://dx.doi.org/10.1002/anie.201205072.

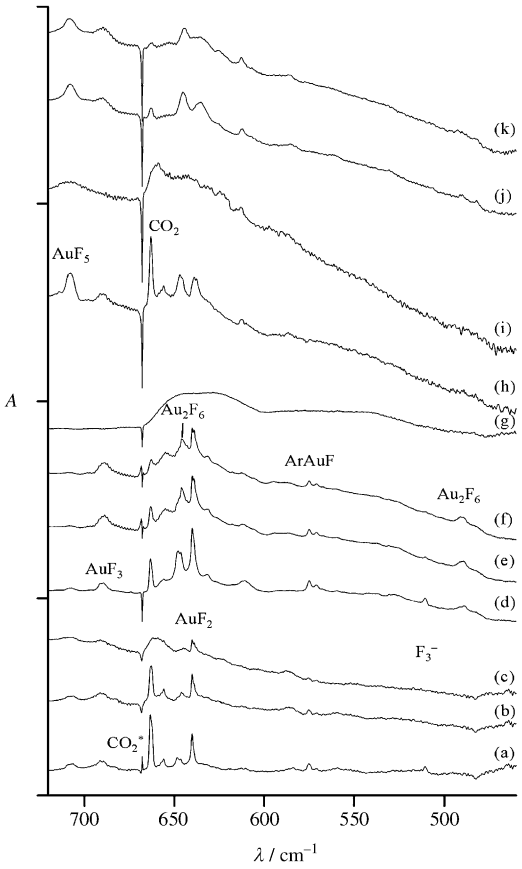

Figure 1. IR spectra from laser-ablated Au atom reactions with F_2 in excess argon co-deposited for 1 h at 4 K in Freiburg. a) Au + F_2 (3%) in Ar, b) after annealing to 20 K, c) after annealing to 30 K; d) Au + F_2 (6%), e) after annealing to 30 K, f) after annealing to 40 K, g) spectrum at 150 K; h) Au + F_2 (12%), i) after annealing to 40 K; j) Au + F_2 (24%), and k) after annealing to 30 K.

Analogous spectra were recorded after sample deposition in neon, Figure 2. As usual for neon matrices, we observed sharper bands. Two remarkable differences appear when the matrix spectra are compared. First, a very strong, sharp band

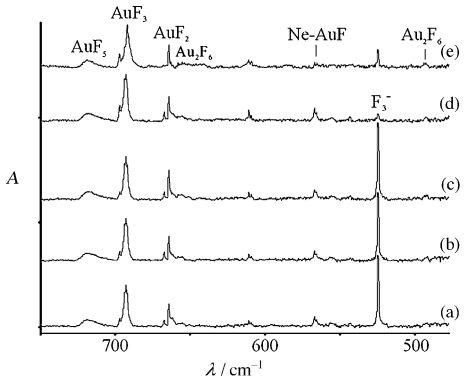

Figure 2. IR spectra from laser-ablated Au atom reactions with F_2 in excess neon at 4 K in Virginia. a) Au + F_2 (0.4%) in Ne co-deposited for 1 h, b) after 15 min > 530 nm irradiation, c) after 15 min > 380 nm irradiation, d) after 15 min 240–380 nm irradiation, e) after annealing to 10 K.

at 524.7 cm^{-1} in neon corresponds to a weaker absorption at 510.6 cm^{-1} in the argon matrix. These bands have been recently assigned to be the isolated trifluoride molecular anion, $[F_3]^-$.[40] Second, the bands at 655 cm^{-1} and 489 cm^{-1} in argon, which increase on annealing, are much weaker in neon, and bands at 655 and 494 cm^{-1} are detected. Furthermore, the neon matrix band does not increase with annealing owing to low accessible temperatures, which do not allow sufficient diffusion of trapped species. Note, neon matrices cannot be annealed much higher than 12 K, whereas solid argon can be sustained above 40 K. Additional neon matrix spectra are shown in the Supporting Information, Figures SI1 and SI2. Again, the spectra recorded at Virginia and Freiburg are essentially the same except for the highest frequency absorption above 700 cm^{-1}.

The bands below 500 cm^{-1} are indicative of bridging fluorine atoms, which is in agreement with our quantum-chemical calculations. The asymmetric bridging fluorine stretching frequency of Au_2F_6 has been calculated to be 508.7, 493.5 cm^{-1} at the SCS-MP2 and SCS-CC2 level where the latter is in excellent agreement with its 494, 489 cm^{-1} observation in neon and argon matrices. Its terminal Au–F stretching frequencies have been computed at 688.9 and 683.9 cm^{-1} at SCS-MP2 and 651.8, 642.7 cm^{-1} at SCS-CC2 level, which match the experimental 655 cm^{-1} value as well (see Table 2 and the Supporting Information). In further support of this assignment is the broad 640 cm^{-1} absorption (Figure 1 g), which is due to the residual gold fluoride species left on the window after the argon matrix has evaporated. This is probably a terminal stretching mode of polymeric AuF_3 which has not been observed in the bulk phase. This is further supported by observation of essentially the same spectrum from heating bulk AuF_3 to 550 °C and depositing the vapor through an unheated stainless steel valve into the matrix (see the Supporting Information).

The rare gases neon and argon show different matrix effects, and these atoms can even interact with the trapped molecules, especially if they are strongly electrophilic like the gold fluorides. The 567.2 cm^{-1} band in neon and the 575.1 cm^{-1} band in argon are due to the Au–F stretching mode for the diatomic AuF molecule in solid matrices (Figures 1 and 2). Additional neon matrix experiments with 1% F_2 doped with 0.1 to 1.0% Ar show only two distinct product absorptions in this region, which suggest that one noble gas atom is strongly involved in the complex formed.

In the gas phase, the diatomic AuF molecule exhibits the fundamental absorption at 557.16 cm^{-1}.[20] Quantum-chemical calculations at the coupled-cluster level predict its stretching frequency in the range from 555 cm^{-1} to 541 cm^{-1} (see Table 2 and the Supporting Information). However as our investigated molecules are trapped in either solid neon or argon, the pure, isolated AuF molecule cannot be produced owing to its relatively strong interaction energies of 46.0 kJ mol^{-1} with argon and 8.6 kJ mol^{-1} with neon (energies for the reaction Ng–AuF → Ng + AuF at the CCSD(T)/aug-cc-pVTZ level; see Table 1). Thermochemical calculations of the metathesis reaction between Ar and Ne show clearly that the preferred product is Ar–AuF by 37.4 kJ mol^{-1}. Furthermore, this interaction energy is in line with our observed matrix shifts

Table 1: Computed thermochemical stability of AuF_2 and NgAuF (Ng = Ne, Ar) in kJ mol^{-1}.[a]

Reaction	CCSD(T)[b]	SCS-CC2[c]	SCS-MP2[c]
$AuF_2 \rightarrow AuF + F$[d]	233.9 (−5.5)	228.6 (−6.6)	225.3
	237.9 (−6.7)	*241.6 (−6.4)*	*237.8*
$2\,AuF_2 \rightarrow AuF + AuF_3$	43.3 (−0.2)	3.6 (−2.2)	33.6
		3.8 (−1.9)	*32.8*
$NeAuF \rightarrow Ne + AuF$[e]	8.6 (−0.1)	5.1 (−1.3)	6.8
	8.9 (−0.1)	*6.3 (−1.6)*	*8.3*
$ArAuF \rightarrow Ar + AuF$[f,g]	46.0 (−1.4)	40.2 (−2.7)	47.3
	48.8 (−1.4)	*48.5 (−2.9)*	*54.7*
$NeAuF + Ar \rightarrow ArAuF + Ne$	−37.4 (1.3)	−35.1 (1.5)	−40.5
	−39.9 (1.3)	*−42.2 (1.2)*	−46.5

[a] Values in normal text style are of triple-ζ basis set quality, whereas values in *italics* are of quadruple-ζ basis set quality. In parentheses are ZPE corrections. [b] aug-cc-pVXZ. [c] def2-XZVPP. [d] 210 kJ mol^{-1} computed at the MP2 level.[17] [e] 8.9 kJ mol^{-1} computed at CCSD/aug-cc-pVQZ[29] and 8.6 kJ mol^{-1} computed at CP-corrected CCSD(T)/CBS.[27] [f] 50.4 kJ mol^{-1} computed at CCSD/aug-cc-pVQZ.[29] [g] 54.3 kJ mol^{-1} computed at CCSD/CBS.[29]

from gas-phase to neon and argon matrix frequencies, which is caused by progressively stronger bonding interactions and ion-induced dipole interactions between AuF and the noble-gas atoms Ne and Ar, respectively. Furthermore, our observation is supported by previous coupled-cluster investigations where this trend was already predicted (Table 2).[26,27,29] However, the 8 cm^{-1} observed difference between the argon and neon matrix frequencies versus the calculated 22 cm^{-1} difference arises because the surrounding argon matrix red-shifts Ar−AuF more than the neon matrix red-shifts Ne−AuF, and this matrix effect decreases the observed difference relative to the computed isolated Ar−AuF and Ne−AuF frequency difference. In fact, the 585.9 cm^{-1} band observed with trace Ar doped in Ne is due to Ar−AuF in solid neon, which is 19 cm^{-1} above Ne−AuF in solid neon, and this difference is in excellent agreement with the above calculated difference.

Table 2: Observed and calculated fundamental frequencies in the Au−F stretching region of gold fluorides and NgAuF compounds (Ng = Ne, Ar)[a]

	Obs. (Ar)	Obs. (Ne)	CCSD(T)/aug-cc-pVXZ[b]	SCS-CC2/def2-XZVPP[b]	SCS-MP2/def2-XZVPP[b]
AuF[c]	–	–	545.8	547.3 (29)	577.1 (58)
			541.3	*554.8 (35)*	*578.5 (63)*
NeAuF[d]	–	567.2	558.5	559.9 (33)	594.1 (59)
			563.9	*571.3 (40)*	*600.5 (64)*
ArAuF[e]	575.1	–	580.7	588.9 (45)	614.8 (62)
			585.4	*591.4 (50)*	*614.4 (65)*
AuF_2[f]	640.1	664.8	647.0	648.1 (179)	662.3 (206)
			650.7	*640.6 (184)*	*654.6 (207)*
AuF_3	690.1	692.4	669.5	656.9 (129)	680.8 (183)
			672.7	*650.4 (134)*	*673.6 (185)*
Au_2F_6	655	655		651–643	688–684
	489	494		*493.5 (272)*	508.7 (334)
AuF_5[g]	720[h]	720[h]	685.5	635.5 (43)	689.0 (98)
	708[i]	711[i]	(104)		*682.4 (100)*

[a] The complete set of calculated frequencies is given in the Supporting Information. Values in parenthesis are intensities in [km mol^{-1}]. [b] Values in normal text style are of triple-ζ basis set quality whereas values in *italics* are of quadruple-ζ basis set quality. [c] Experimental gas-phase value 563.7 cm^{-1};[20] values from other calculations at DC-CCSD(T) level: 575 cm^{-1},[26] 555 cm^{-1},[41] 560 cm^{-1}.[42] [d] CCSD/aug-cc-pVQZ 579.5 cm^{-1};[29] CCSD(T)/V5Z 577 cm^{-1}.[27] [e] CCSD/aug-cc-pVQZ 597.6 cm^{-1}.[29] [f] SOS-MP2/def2-TZVPP 644.4 cm^{-1}; SOS-MP2/def2-QZVPP 636.9 cm^{-1}. [g] Values at MP2/def2-TZVPP (see the Supporting Information). [h] Measured in Virginia. [i] Measured in Freiburg.

The sharp, strong bands at 640.1 cm^{-1} in argon and 664.8 cm^{-1} in neon bracket our CCSD(T)/aug-cc-pVTZ frequency calculations for the linear AuF_2 molecule (calculated in C_{2v} symmetry, SOMO A_{1g}), which has a computed asymmetric frequency in the 640–650 cm^{-1} range (Table 2 and the Supporting Information). Furthermore, the intensity profile of the observed bands increases in the order of Ar−AuF, AuF_2, AuF_3,and AuF_5 as the F_2 concentration is increased stepwise from 0.4 to 4% in Virginia and 3 to 24% in Freiburg. Furthermore, the strong AuF_2 absorption frequency correlates nicely with those for AgF_2 and CuF_2, which show resolved natural metal isotopic splitting (Supporting Information, Figure SI3). The formation of the new Au^{II} molecule AuF_2 is also supported by its thermochemical stability where homolytic bond breaking is computed to be endothermic by 233.9 kJ mol^{-1} at the CCSD(T)/aug-cc-pVTZ level. Furthermore, its disproportionation reaction $2\,AuF_2 \rightarrow AuF + AuF_3$ is endothermic as well by 43.3 kJ mol^{-1} at the same computational level. Our computed thermochemical stability of the AuF_2 molecule is sufficient for trapping this species at cryogenic conditions in rare-gas matrices, particularly from the $Au + F_2$ reaction in the presence of condensing noble gas to quench reaction exothermicity.

The next experimental absorptions to increase with fluorine concentration, the bands at 690.1 cm^{-1} in Ar and 692.4 cm^{-1} in Ne, can be assigned to AuF_3. Our CCSD(T)/aug-cc-pVTZ calculations show that AuF_3 has a T-shaped structure owing to first-order Jahn–Teller distortion (Figure 3), which results in two different Au–F stretching modes: one at 669.5 cm^{-1} (F−Au−F mode) and a very weak one at 612.2 cm^{-1} (Au < C- < F mode), which cannot be observed here. This calculation, together with observation of the dimerization process during the annealing, allows a confident assignment of the AuF_3 molecule and its dimer Au_2F_6.

Apart from its laser-ablation preparation, we have produced polymeric AuF_3 in bulk quantities. The Raman spectrum identifies the product to be pure solid AuF_3 (Supporting Information, Figure SI4). Several attempts were made to evaporate this material into the matrix to detect the monomeric AuF_3 in the IR spectra. Unfortunately, only polymeric Au_nF_m species with one terminal Au−F (654, 660 cm^{-1}) and one bridging Au–F–Au band (478, 476 cm^{-1}) could be detected in neon or argon (Supporting Information, Figure SI5). In previous mass spectrometric studies, it was found that the vapor contains AuF_3, Au_2F_6, and Au_3F_9 and at higher temperatures the lower fluorides are favored.[2,43]

The highest observed frequency in our matrix-isolation experiments is a broad band at 720 cm^{-1} (708 cm^{-1} Freiburg) in argon and a sharper 720 cm^{-1} (711 cm^{-1} Freiburg) absorption in neon, and we assign these bands tentatively to AuF_5 for the following reasons. We have noticed that these bands occur only if higher fluorine concentrations are involved and after the formation of AuF_2 and AuF_3. Although AuF_5 is

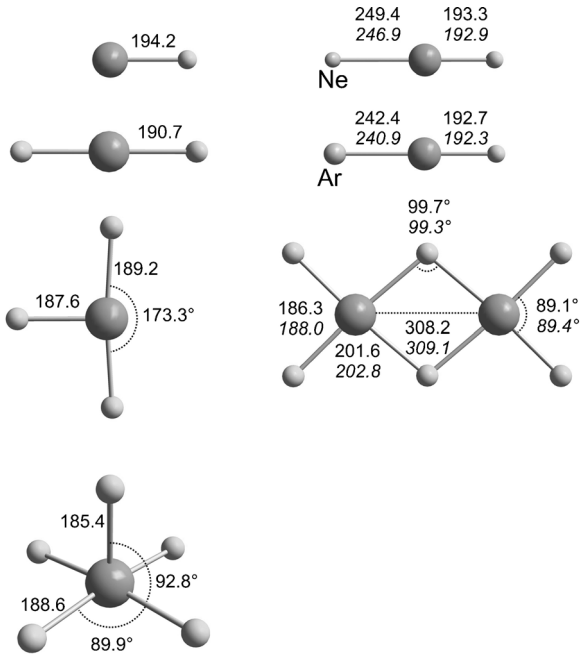

Figure 3. Optimized structures of gold fluorides and noble-gas gold fluorides at different levels of theory. AuF, AuF_2, AuF_3, and NgAuF (Ng = Ne, Ar) are computed at the CCSD(T)/aug-cc-pVTZ level, *italics* at CCSD(T)/aug-cc-pVQZ, and Au_2F_6 are computed at SCS-MP2/def2-TZVPP and in *italics* the SCS-CC2/def2-TZVPP level.[45–49]

a stable known species, no IR spectra have been recorded for the bulk material. This is most likely due to its strong oxidizing power. Gold pentafluoride has so far only been vibrationally characterized by Raman spectroscopy, because handling the bulk material and its spectroscopic characterization can be done in the same glass vessel.[9,44] Reliable experimental IR spectra are therefore not available for comparison. However, a previous validation of DFT and MP2 frequency calculations on the experimental Raman spectra have shown that the highest frequencies at B3LYP (11 cm^{-1}) and MP2 (6 cm^{-1}) are very close to experiment.[11] We therefore believe that our computed frequencies at SCS-MP2/def2-TZVPP 689 cm^{-1} and CCSD(T)/aug-cc-pVTZ of 685.5 cm^{-1} (Table 2 and the Supporting Information) supports the identification of monomeric AuF_5, as our calculated frequencies fall below the experimental values. To the best of our knowledge, no monomeric AuF_5 has been characterized before this work, which is due to its ability to form dimers and trimers.[14]

In conclusion, matrix-isolation experiments using neon and argon show IR absorptions that are due to the gold fluoride molecules AuF_2, AuF_3, Au_2F_6, and AuF_5 as well as the noble gas gold fluorides Ne–AuF and Ar–AuF. These assignments are based on fluorine concentration dependence as well as correlation with coupled-cluster calculated frequencies. Similar work in progress with OF_2 yields only the lower three fluoride species. Note that the argon-to-neon matrix shift is larger for the lower fluorides as more of the metal center is exposed for this matrix interaction. The characterization of AuF_2 is remarkable, because this species is the first observed binary open-shell and Au^{II} gold fluoride species. Furthermore, this work reports evidence for monomeric molecular AuF_5 for the first time.

These assignments are supported by quantum-chemical calculations at the CCSD(T) level, which indicate the thermochemical stability of AuF_2 against homolytic bond breaking and disproportionation. Furthermore, we have observed the first Ne–AuF compound together with its known heavier homologue Ar–AuF through their Au–F stretching modes. In conjunction with previous quantum-chemical calculations, we observed a stronger Au–F bond in Ar–AuF than in Ne–AuF owing to its higher matrix Au–F frequency.

We believe that these new reaction products are ideal calibration points for further quantum-chemical investigations of gold compounds. Such investigations of gold bearing molecules are ongoing in our groups.

Received: June 28, 2012
Published online: September 23, 2012

Keywords: fluorine · gold fluorides · high oxidation states · matrix-isolation spectroscopy · noble-gas species

[1] H. Moissan, *Compt. Rend.* **1889**, *109*, 807.
[2] B. Réffy, M. Kolonits, A. Schulz, T. M. Klapötke, M. Hargittai, *J. Am. Chem. Soc.* **2000**, *122*, 3127.
[3] F. W. B. Einstein, R. P. Rao, J. Trotter, N. Bartlett, *J. Chem. Soc. A* **1967**, 478.
[4] A. G. Sharpe, *J. Chem. Soc.* **1949**, 2901.
[5] I. C. Tornieporth-Oetting, T. M. Klapötke, *Chem. Ber.* **1995**, *128*, 957.
[6] P. Schwerdtfeger, P. D. W. Boyd, S. Brienne, A. K. Burrell, *Inorg. Chem.* **1992**, *31*, 3411.
[7] A. Schulz, M. Hargittai, *Chem. Eur. J.* **2001**, *7*, 3657.
[8] B. Zemva, K. Lutar, A. Jesih, W. J. Casteel, Jr., A. P. Wilkinson, D. E. Cox, R. B. Von Dreele, H. Borrmann, N. Bartlett, *J. Am. Chem. Soc.* **1991**, *113*, 4192.
[9] I.-C. Hwang, K. Seppelt, *Angew. Chem.* **2001**, *113*, 3803; *Angew. Chem. Int. Ed.* **2001**, *40*, 3690.
[10] J. Brunvoll, A. A. Ischenko, A. A. Ivanov, G. V. Romanov, V. B. Sokolov, V. P. Spiridonov, T. G. Strand, *Acta Chem. Scand. A* **1982**, *36*, 705.
[11] S. Riedel, M. Kaupp, *Inorg. Chem.* **2006**, *45*, 1228.
[12] P. Pyykkö, J. P. Desclaux, *Acc. Chem. Res.* **1979**, *12*, 276.
[13] P. Pyykkö, *Chem. Rev.* **1988**, *88*, 563.
[14] S. Riedel, M. Kaupp, *Coord. Chem. Rev.* **2009**, *253*, 606.
[15] A. A. Timakov, V. N. Prusakov, Y. V. Drobyshevskii, *Dokl. Akad. Nauk SSSR* **1986**, *291*, 125.
[16] D. Himmel, S. Riedel, *Inorg. Chem.* **2007**, *46*, 5338.
[17] P. Schwerdtfeger, J. S. McFeaters, M. J. Liddell, J. Hrusak, H. Schwarz, *J. Chem. Phys.* **1995**, *103*, 245.
[18] P. Schwerdtfeger, J. S. McFeaters, R. L. Stephens, M. J. Liddell, M. Dolg, B. A. Hess, *Chem. Phys. Lett.* **1994**, *218*, 362.
[19] D. Schröder, J. Hrusak, I. C. Tornieporth-Oetting, T. M. Klapötke, H. Schwarz, *Angew. Chem.* **1994**, *106*, 223.
[20] T. Okabayashi, Y. Nakaoka, E. Yamazaki, M. Tanimoto, *Chem. Phys. Lett.* **2002**, *366*, 406.
[21] C. J. Evans, M. C. L. Gerry, *J. Am. Chem. Soc.* **2000**, *122*, 1560.
[22] J. M. Thomas, N. R. Walker, S. A. Cooke, M. C. L. Gerry, *J. Am. Chem. Soc.* **2004**, *126*, 1235.
[23] S. A. Cooke, M. C. L. Gerry, *J. Am. Chem. Soc.* **2004**, *126*, 17000.
[24] C. J. Evans, D. S. Rubinoff, M. C. L. Gerry, *Phys. Chem. Chem. Phys.* **2000**, *2*, 3943.

[25] S. M. Beyhan, A. W. Goetz, C. R. Jacob, L. Visscher, *J. Chem. Phys.* **2010**, *132*, 044114.
[26] L. Belpassi, I. Infante, F. Tarantelli, L. Visscher, *J. Am. Chem. Soc.* **2008**, *130*, 1048.
[27] W. Zou, Y. Liu, J. E. Boggs, *Chem. Phys. Lett.* **2009**, *482*, 207.
[28] T.-Y. Lai, C.-Y. Yang, H.-J. Lin, C.-Y. Yang, W.-P. Hu, *J. Chem. Phys.* **2011**, *134*, 244110.
[29] C. J. Evans, T. G. Wright, A. M. Gardner, *J. Phys. Chem. A* **2010**, *114*, 4446.
[30] P. Pyykkö, *Chem. Soc. Rev.* **2008**, *37*, 1967.
[31] P. Pyykkö, *Inorg. Chim. Acta* **2005**, *358*, 4113.
[32] P. Pyykkö, *Angew. Chem.* **2004**, *116*, 4512; *Angew. Chem. Int. Ed.* **2004**, *43*, 4412.
[33] F. Mohr, *Gold Bull.* **2004**, *37*, 164.
[34] S. H. Elder, G. M. Lucier, F. J. Hollander, N. Bartlett, *J. Am. Chem. Soc.* **1997**, *119*, 1020.
[35] I.-C. Hwang, K. Seppelt, *Z. Anorg. Allg. Chem.* **2002**, *628*, 765.
[36] L. Andrews, X. Wang, L. Manceron, K. Balasubramanian, *J. Phys. Chem. A* **2004**, *108*, 2936.
[37] X. Wang, L. Andrews, *J. Phys. Chem. A* **2010**, *114*, 2293.
[38] L. Andrews, *Chem. Soc. Rev.* **2004**, *33*, 123.
[39] L. Andrews, A. Citra, *Chem. Rev.* **2002**, *102*, 885.
[40] S. Riedel, T. Köchner, X. Wang, L. Andrews, *Inorg. Chem.* **2010**, *49*, 7156.
[41] M. Iliaš, P. Furdik, M. Urban, *J. Phys. Chem. A* **1998**, *102*, 5263.
[42] C. Puzzarini, K. A. Peterson, *Chem. Phys.* **2005**, *311*, 177.
[43] N. S. Chilingarov, M. V. Korobov, S. V. Rudometkin, A. S. Alikhanyan, L. N. Sidorov, *Int. J. Mass Spectrom. Ion Processes* **1986**, *69*, 175.
[44] M. J. Vasile, T. J. Richardson, F. A. Stevie, W. E. Falconer, *J. Chem. Soc. Dalton Trans.* **1976**, 351.
[45] SCS-MP2: S. Grimme, *J. Chem. Phys.* **2003**, *118*, 9095.
[46] SCS-CC2: A. Hellweg, S. A. Gruen, C. Hättig, *Phys. Chem. Chem. Phys.* **2008**, *10*, 4119.
[47] CC2: C. Hättig, *J. Chem. Phys.* **2003**, *118*, 7751.
[48] MP2/CC2: Turbomole 6.2, University of Karlsruhe and Forschungszentrum Karlsruhe GmbH, Karlsruhe, **2011**; http://www.turbomole.com.
[49] CCSD(T): H.-J. Werner, P. J. Knowles, R. Lindh, F. R. Manby, M. Schütz, P. Celani, T. Korona, G. Rauhut, R. D. Amos, A. Bernhardsson, A. Berning, D. L. Cooper, M. J. O. Deegan, A. J. Dobbyn, F. Eckert, C. Hampel, G. Hetzer, A. W. Lloyd, S. J. McNicholas, W. Meyer, M. E. Mura, A. Nicklaß, P. Palmieri, R. Pitzer, U. Schumann, H. Stoll, A. J. Stone, R. Tarroni, T. Thorsteinsson, MOLPRO 2006.1 ed., Birmingham, UK, **2006**.

